

Period Multiplication in a Continuous Time Series of Radio-Frequency DBDs at Atmospheric Pressure

Jiao Zhang, Yanhui Wang* and Dezhen Wang

State Key Laboratory of Materials Modification by Laser, Electron, and Ion Beams, School of Physics and Optoelectronic Technology, Dalian University of Technology, Dalian 116024, China.

Received 15 July 2010; Accepted (in revised version) 5 November 2010

Communicated by Zhengming Sheng

Available online 29 November 2011

Abstract. As a spatially extended dissipative system with strong nonlinearity, the radio-frequency (rf) dielectric-barrier discharges (DBDs) at atmospheric pressure possess complex spatiotemporal nonlinear behaviors. In this paper, the time-domain nonlinear behaviors of rf DBD in atmospheric argon are studied numerically by a one-dimensional fluid model. Simulation results show that, under appropriate controlling parameters, the rf DBD can undergo a transition from single-period state to chaos through period doubling bifurcation with increasing discharge time, i.e., the regular periodic oscillation and chaos can coexist in a long time series of the atmospheric-pressure rf DBD. With increasing applied voltage amplitude, the duration of the periodic oscillation reduces gradually and chaotic zone increases, and finally the whole discharge series becomes completely chaotic state. This is different from conventional period doubling route to chaos. Moreover, the spatial characteristics of rf period-doubling discharge and chaos, as well as the parameter range of various discharge behaviors occurring are also investigated in this paper.

PACS: 52.35.Kw, 52.65.Kj, 52.80.Pi

Key words: Atmospheric radio-frequency discharge, period-doubling bifurcation, chaos.

1 Introduction

Recently, there has been growing concern about radio-frequency atmospheric pressure glow discharges (APGDs) that benefit many industrial fields [1–5] for its removing of vacuum chamber and its capability of offering non-equilibrium plasma. A large number of experimental and numerical works have been carried out to investigate the modes of

*Corresponding author. *Email addresses:* summer_j@yahoo.cn (J. Zhang), yanhui-w@sohu.com (Y. Wang), wangdez@dlut.edu.cn (D. Wang)

rf APGD and their influence on plasma stability [6–8]. Commonly, in higher discharge current radio-frequency APGDs are unstable and easy to evolve into arc plasma. One of the effective solutions to prevent the glow-to-arc transition is employing dielectrically insulated electrodes to control the unlimited growth of discharge current [8]. This means radio-frequency dielectric barriers discharge (DBD) can provide stable glow plasma at high discharge current and therefore have more extensive application prospects.

As the most familiar route to chaos, period multiplication theory has been applied to various areas like laser system [9], plasma [10–16] and so on. Using iteration method, the equation solution can be in order or out of order corresponding to different coefficients, for example, the famous Logistic map. DBD system is a spatially extended dissipated system with strong nonlinearity. Under appropriate operation conditions, various oscillations and instabilities could occur in this discharge system. Pervious investigations have shown that period multiplication and chaotic phenomena have been observed in atmospheric-pressure DBD operating at kilohertz frequency range [15, 16]. These nonlinear behaviors appearing in atmospheric-pressure DBD could change the plasma structure and affect plasma stability. Therefore it is important to study the nonlinear behaviors in radio-frequency DBD, not only to improve plasma stability but also to control rf APGD operation modes in different modes to meet different application requirements.

The aim of the present work is to study numerically the transition from periodic discharge to chaos occurring in a continuous time series of rf DBD in atmospheric argon, as well as their parameter dependence based on a one-dimensional fluid model.

2 Model

Present study is based on a one-dimensional, self-consistent fluid model developed for APGD that has been used in previous studies [15–17]. The rf DBD is generated between two dielectrically insulated parallel-plate electrodes connected externally to a sinusoidal voltage. The work gas is pure argon. To focus on temporal nonlinear behaviors of rf DBD, complex chemical processes are ignored and only direct ionization and recombination processes are considered. Since the electrode gap size is much smaller than the width of the electrode, we assume that the atmospheric DBD under study maintains uniform in the direction perpendicular to that of the externally applied voltage. The diffusion-drift approximation is used. Hydrodynamics equations are used to describe the temporal evolution of rf DBD. The densities of argon ions and electrons are described by continuity equations, which are as follows:

$$\frac{\partial n_e}{\partial t} + \frac{\partial j_e}{\partial x} = S_e, \quad (2.1a)$$

$$\frac{\partial n_p}{\partial t} + \frac{\partial j_p}{\partial x} = S_p, \quad (2.1b)$$

where t and x are the time and interelectrode axial distance, respectively. n_e and n_p represent densities of electron and ion, respectively. j_e and j_p represent flux densities of

electron and ion, respectively. S_e and S_p are source terms for electron and ion, in which only direct impact ionization and combination in the bulk of the gas gap are taken into account. Ionization and combination coefficients are used in [18,19]. j_e and j_p are deduced by momentum equation:

$$j_e(x,t) = -\mu_e n_e(x,t)E(x,t) - D_e \frac{\partial n_e(x,t)}{\partial x}, \quad (2.2a)$$

$$j_p(x,t) = \mu_p n_p(x,t)E(x,t) - D_p \frac{\partial n_p(x,t)}{\partial x}, \quad (2.2b)$$

where D_e and D_p are diffusion coefficients for electron and ion. Their values are taken from [20]. The expression of electric field is presented by current conservation equation which is deduced from Poisson equation.

$$\epsilon_0 \epsilon(x) \frac{\partial E(x,t)}{\partial t} + i_c(x,t) = i_T(x,t), \quad (2.3)$$

where i_c is conduction current density and i_T is discharge current density. $\epsilon(x)$ is a piecewise function of interelectrode position, and its value is either 1 in gas gap or ϵ_B in dielectric layers. The expression of the conduction current density is $i_c = q(j_p + j_e)$, where q is the electronic charge. Secondary electron emission from the instantaneous cathode is considered here for ion bombardment alone, and therefore the electron flux leaving the cathode is taken as γj_p . Here γ is the secondary electron emission coefficient. Its value is set to 0.01.

The expression of total current density is obtained by integrating Eq. (2.3) between the metallic electrodes.

$$i_T(t) = \left[\int_{x_1}^{x_2} i_c(x,t) dx - \epsilon_0 \frac{\partial V(t)}{\partial t} \right] d^{-1}, \quad (2.4a)$$

$$d = 2 \frac{d_B}{\epsilon_B} + d_g, \quad (2.4b)$$

where d_B is the thickness of dielectric barrier layers, and d_g is gap distance. Radio-frequency sinusoidal voltage of $V(t) = V_a \sin(2\pi ft)$ is applied.

An autonomous set of differential equations with the general form of $dx_i/dt = f_i(x_i)$ is formed by partial differential Eqs. (2.1a) and (2.1b) (regardless of partial derivative of space), together with ordinary differential Eq. (2.4a), where x_i ($i = 1, 2, 3$), represent three variables, corresponding to n_e , n_p and E , respectively. Equations of such form have been well investigated and shown to display chaotic behavior [13]. The sinusoidal source applied to equation Eq. (2.3) as an oscillating element also increases the freedom degree of the model, making all the variables periodic oscillating.

The above set of equations can be solved by semi-implicit Scharfetter-Gummer scheme. Eqs. (2.1a) and (2.1b) are one-dimensional parabolic equations substituted by Eqs. (2.2a) and (2.2b), and a tridiagonal matrix about particle density will be obtained. A detailed description of the model can be found in [21].

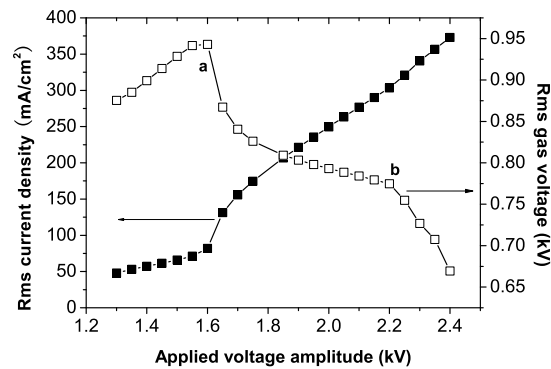


Figure 1: Current-voltage characteristic of applied voltage amplitude and rms current density as well as rms gas voltage.

3 Results and discussion

The model is performed for a 13.56MHz DBD, and each electrode is covered by a dielectric layer of 1mm with the dielectric permittivity of 7.5. The gas gap is 3mm. According to previous reports [6–8], the discharge behaviors are closely related to their current-voltage characteristics, and those complex nonlinear behaviors always accompany with negative differential conductivity. Current-voltage characteristics of rf DBD in argon is shown in Fig. 1, where the relationship between applied voltage amplitude and the rms gas voltage, as well as the rms current density are plotted. It is worth mentioning that 5000 rf periods is iterated for each point. It is clear that two different regimes of atmospheric pressure rf glow discharge can be identified. When the applied voltage amplitude is less than 1.6kV at *a*-point, as the applied voltage amplitude increases, rms current density increases, and corresponding rms gas voltage also increases, suggesting the whole discharge system have a positive differential resistance. When the applied voltage amplitude is more than 1.6kV, the gas voltage starts to decrease with increasing applied voltage, whereas the current density grows continuously in Fig. 1, indicating the other regime with negative differential resistance. It is worth noting that with the increase of applied voltage amplitude, the value of negative differential resistance also varies and above 2.2kV at *b*-point, the negative differential resistance becomes much larger, which indicates more complex dynamical behaviors existing in this region. Our study would be focused on this region with bigger negative differential resistance.

Previous studies [17] concerning period multiplication and discharge characteristics in atmospheric rf discharge reported that by increasing the radio-frequency sinusoidal voltage amplitude while keeping other discharge parameters constant, the rf DBD in argon undergoes a transition from single-period discharge to chaos through period doubling bifurcation. This process is the well-known period doubling route to chaos. The amplitude of applied voltage is an important parameter controlling the discharge bifurcation. However, in this DBD system, when applied voltage amplitude is set as 2350V,

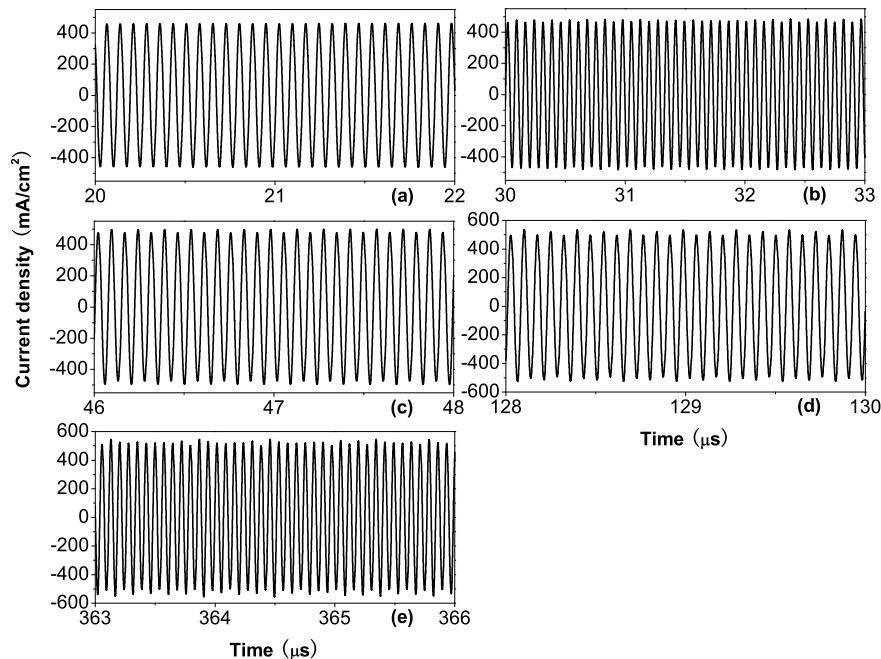


Figure 2: Period doubling bifurcation and chaos in a continuous time series of rf DBD. (a) single period discharge, (b) unstable period-2 state, (c) period-2 state, (d) period-4 state, and (e) chaos.

with increasing discharge time, the discharge can also undergo a transition from single-period state to chaos through period doubling bifurcation. This is shown in Fig. 2, where different bifurcation states are identified in different time ranges. The discharge is first stabilized at single period discharge, in which discharge current density has the same periodicity with applied voltage, see Fig. 2(a). As discharge process goes on above $22.12\mu\text{s}$, the discharge becomes irregular and bifurcates into an unstable period-2 state in Fig. 2(b). It can be seen that the discharge fluctuates intermittently from one kind of period-2 state to another with discharge time being prolonged. Until $42.04\mu\text{s}$, the discharge comes into typical period-2 state, as shown in Fig. 2(c), in which the period of discharge current density is twice as that of applied voltage and a strictly alternating series of strong and weak current peaks can be observed. This period-2 state sustains about 610 periods of applied voltage and then at $87.46\mu\text{s}$ the discharge bifurcates into period-4 state. In period-4 state, temporal profile of discharge current repeats every four cycles of applied voltage, as shown in Fig. 2(d). Period-4 state possesses about 1200 periods of applied voltage. Finally, discharge evolves into chaos at $171.83\mu\text{s}$, as shown in Fig. 2(e), where the discharge current density fluctuates stochastically, and discharge system is out of order. This discharge process well performs the period doubling bifurcation and chaos in a continuous time series, i.e., period multiplication and chaos can coexist in a long time series of the atmospheric rf DBD. It is worth mentioning that in the whole evolution process, discharge current density has a slight increase.

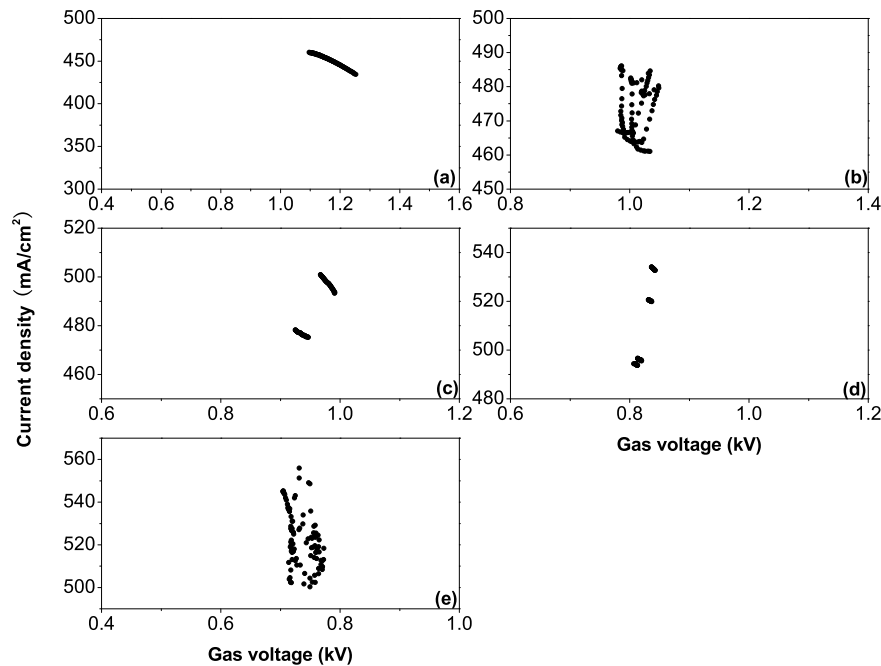


Figure 3: Poincaré sections corresponding to Fig. 2. (a) single period discharge from the 200th period to the 300th period, (b) unstable period-2 state from the 400th period to the 500th period, (c) stable period-2 state from the 600th period to the 700th period, (d) period-4 state from the 1700th period to the 1800th period, and (e) chaotic state from the 4900th period to the 5000th period.

In order to identify exactly each bifurcation state, Fig. 3 gives the Poincaré sections of the above bifurcation sequence. Poincaré sections are formed through the intersections of phase space trajectories with an arbitrary plane. Each Poincaré section plotted in Fig. 3 contains data of 100 cycles of the applied voltage. For the single period discharge, the Poincaré section is a short line, not a strict dot because of the slight increase of current density with discharge time, see Fig. 3(a). Fig. 3(b) shows the Poincaré section of unstable period-2 state, where the dots are mainly concentrated in two regions due to the fluctuation of period-two state. In typical period-2 state, the resultant Poincaré map contains two fixed short line segment, see Fig. 3(c). Then, four fixed points appearing in Poincaré section, which indicates clearly the discharge is period-4 state, see Fig. 3(d). In Fig. 3(e), the Poincaré map consists of randomly scattered points, which means the discharge has entered into chaotic state.

Further simulations show that with the increase of applied voltage, periodic oscillation reduces, and chaotic zone increases, finally, discharge comes into chaos completely. This can be observed from Fig. 4, where the bifurcation diagrams with discharge time under different applied voltages are given. For the single period discharge, only one current peak value is produced at one fixed time. In the unstable period-2 region multiple current peak values emerge at each time. The operation domain with two current peak values at one period corresponds to stable period-2 state, and two pitchfork doubling

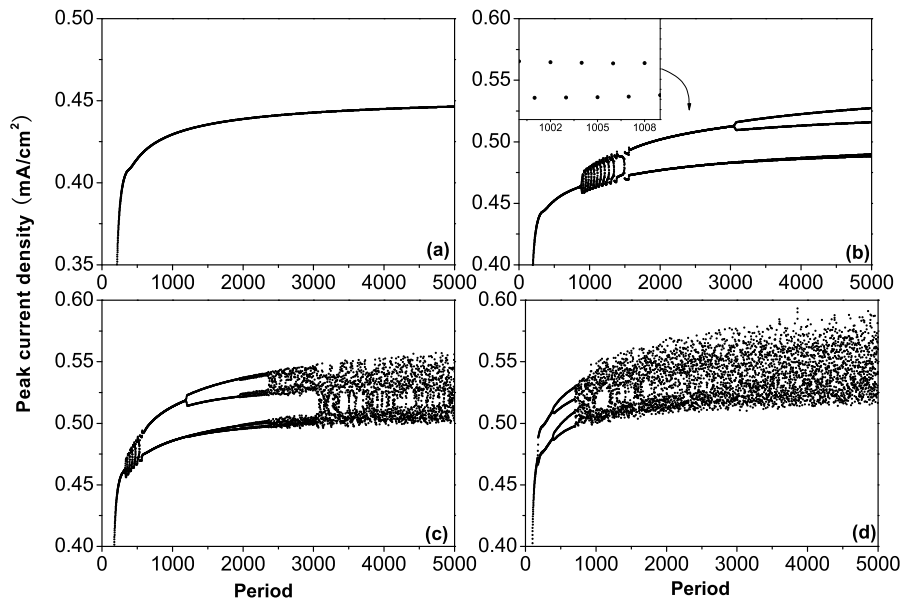


Figure 4: Bifurcation diagrams of the relation between period and peak current density. (a) 2200V; (b) 2300V; (c) 2350V; and (d) 2400V.

sequences correspond to period-4 state. In the chaotic domain, a large number of current peak values appear at one fixed time. When the applied voltage amplitude is 2200V, the discharge is single period state within 5000 periods, see Fig. 4(a). The peak current density increases smoothly with the discharge time. With increasing applied voltage, the time of single period discharge is shortened and the unstable $2p$ occupies 730 periods from the 860th period to the 1590th period before period-2 state. After about the 3340th period, discharge becomes stable period-4 state, see Fig. 4(b). Since the two low current peak values are almost equal, the two lines are superposed. When applied voltage amplitude is set as 2350V, periodic oscillation reduces distinctly. At about the 500th period, unstable period-2 state has been observed. Total period-2 (including unstable period-2 state) sustains about 900 periods and period-4 state sustains 740 periods. Chaotic state appears after the 3000th period, see Fig. 4(c). When applied voltage amplitude reaches 2400V, chaos occupies most of discharge time as shown in Fig. 4(d). Continuing to increase applied voltage, period oscillation vanishes, and the discharge becomes chaos completely.

More detailed calculations show that the bifurcations appearing in a continuous time series of rf DBD mainly occur in sheath region. Fig. 5 gives the spatiotemporal evolution of electron density at the applied voltage amplitude of 2350V. The moment that current density reaches its maximum in each period is chosen to plot the spatial profile of electron density, namely, each period corresponds to a line of electron density distribution in gas gap. Different bifurcation states can be identified in Fig. 5(a)-(e). Bifurcations almost occur in sheath region, since the electron density has little change in the bulk-plasma at each bifurcation state, and yet the electron density distribution in sheath exhibits visible

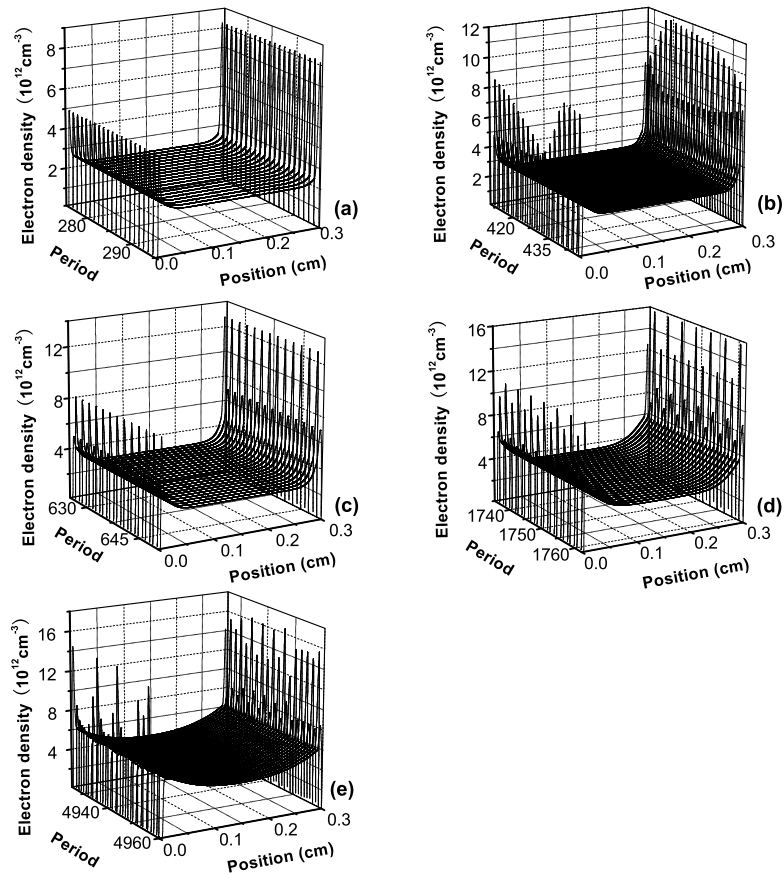


Figure 5: Spatiotemporal profile of electron density at (a) from the 271st to the 298th period, (b) from the 406th to the 447th period, (c) from the 623rd to the 650th period, (d) from the 1735th to the 1762nd period, and (e) from the 4922nd to the 4962nd period.

bifurcation. This indicates that sheath characteristics may be responsible for the complex nonlinear behaviors. From Fig. 5, it is also can be seen that electron density in bulk-plasma is slightly increasing from single period to chaos. It may say that, as the discharge is carried out, more electrons are accumulated by ionizing, leading to the increase of total electron density, and finally cause the bifurcation in sheath. In addition, further simulations reveal that all the bifurcation states in a continuous time series, both period multiplication state and chaotic state, always remain glow-plasma features. Fig. 6 shows spatial evolutions of electron density, ion density and electron field at chaos at the peak current of the 4500th period with voltage amplitude of 2350V. Two regions including sheath region and bulk-plasma region can be observed clearly in Fig. 6. In sheath region, electric field reaches maximum, then decreases linearly, and the ion density is much higher than electrons. In Bulk-plasma region, the densities of ions and electrons are almost the same.

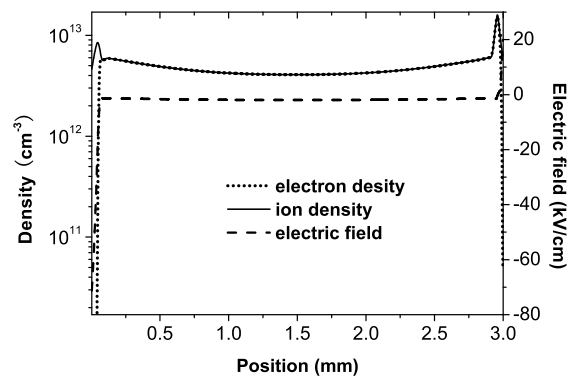


Figure 6: Spatial evolutions of electron density, ion density and electron field at the peak current of the 4500th period with voltage amplitude of 2350V.

4 Conclusions

Based on a one-dimensional fluid model, we have studied period multiplication and chaotic behaviors in a continuous time series of radio-frequency DBD in atmospheric argon. In proper controlling parameters, discharges are able to bifurcate into period-2 state, period-4 state, and chaotic state with increasing discharge time. The bifurcation diagrams under different applied voltage amplitudes show with the increase of voltage amplitude, the duration of the periodic oscillation reduces gradually until the whole time series of the discharge becomes completely chaotic state. The bifurcations appearing in a continuous time series of rf DBD mainly occur in sheath region indicating that sheath characteristics may be responsible for the complex nonlinear behaviors. Spatial evolutions of electron density, ion density and electron field show all the bifurcation states in a continuous time series, both period multiplication and chaotic discharge, always remain glow-plasma features.

Acknowledgments

This work was supported by the National Natural Science Foundation of China under Grant No. 10775026 and 50537020 and Science Research Foundation of Dalian University of Technology.

References

- [1] J. R. Roth, J. Rahel, X. Dai and D. M. Sherman, The physics and phenomenology of one atmosphere uniform glow discharge plasma (*OAugDPTM*) reactors for surface treatment applications, *J. Phys. D: Appl. Phys.*, 38 (2005), 555–567.
- [2] S. Y. Moon, W. Choe and B. K. Kang, A uniform glow discharge plasma source at atmospheric pressure, *Appl. Phys. Lett.*, 84 (2004), 188–190.

- [3] E. Stoffels, A. J. Flikweert, W. W. Stoffels and G. M. W. Kroesen, Plasma needle: a non-destructive atmospheric plasma source for fine surface treatment of (bio)materials, *Plasma Sources Sci. Technol.*, 11 (2002), 383–388.
- [4] Y. -B. Guo and F. C.-N. Hong, Radio-frequency microdischarge arrays for large-area cold atmospheric plasma generation, *Appl. Phys. Lett.*, 82 (2003), 337–339.
- [5] Y. Takao and K. Ono, A miniature electrothermal thruster using microwave-excited plasmas: a numerical design consideration, *Plasma Sources Sci. Technol.*, 15 (2006), 211–227.
- [6] J. J. Shi and M. G. Kong, Mechanisms of the and modes in radio-frequency atmospheric glow discharges, *J. Appl. Phys.*, 97 (2005), 023306.
- [7] J. J. Shi and M. G. Kong, Mode characteristics of radio-frequency atmospheric glow discharges, *IEEE T. Plasma Sci.*, 33 (2005), 624–630.
- [8] J. J. Shi, D. W. Liu and M. G. Kong, Plasma stability control using dielectric barriers in radio-frequency atmospheric pressure glow discharges, *Appl. Phys. Lett.*, 89 (2006), 081502.
- [9] C. Letellier, M Bennoud and G. Martel, Intermittency and period-doubling cascade on tori in a bimode laser model, *Chaos, Solitons and Fractals*, 33 (2007), 782–794.
- [10] T. Braun, J. A. Lisboa and R. E. Francke, Observation of deterministic chaos in electrical discharges in gases, *Phys. Rev. Lett.*, 59 (1987), 613–616.
- [11] P. Y. Cheung and A. Y. Wong, Chaotic behavior and period doubling in plasmas, *Phys. Rev. Lett.*, 59 (1987), 551–554.
- [12] F. Greiner, T. Klinger, H. Klostermann and A. Piel, Experiment and particle-in-cell simulation on self-oscillations and period doubling in thermionic discharge at low pressure, *Phys. Rev. Lett.*, 70 (1993), 3071–3074.
- [13] T. Hayashi, Mixed-mode oscillations and chaos in a glow discharge, *Phys. Rev. Lett.*, 84 (2000), 3334–3337.
- [14] D. D. Šijačić, U. Ebert and I. Rafatov, Period doubling cascade in glow discharges: local versus global differential conductivity, *Phys. Rev. E*, 70 (2004), 056220.
- [15] Y. H. Wang, Y. T. Zhang, D. Z. Wang and M. G. Kong, Period multiplication and chaotic phenomena in atmospheric dielectric-barrier glow discharges, *Appl. Phys. Lett.*, 90 (2007), 071501.
- [16] H. Shi, Y. H. Wang and D. Z. Wang, Nonlinear behavior in the time domain in argon atmospheric dielectric-barrier discharges, *Phys. Plasmas*, 15 (2008), 122306.
- [17] J. Zhang, Y. H. Wang and D. Z. Wang, Numerical study of period multiplication and chaotic phenomena in an atmospheric radio-frequency discharge, *Phys. Plasmas*, 17 (2010), 043507.
- [18] A. L. Ward, Calculations of cathode-fall characteristics, *J. Appl. Phys.*, 33 (1962), 2789–2794.
- [19] M. Moravej, X. Yang, M. Barankin, J. Penelon, S. E. Babayan and R. F. Hicks, Properties of an atmospheric pressure radio-frequency argon and nitrogen plasma, *Plasma Sources Sci.*, 15 (2006), 204–210.
- [20] A. D. Richards, B. E. Thompson and H. H. Sawin, Continuum modeling of argon radio frequency glow discharges, *Appl. Phys. Lett.*, 50 (1987), 492–494.
- [21] Y. H. Wang and D. Z. Wang, Influence of impurities on the uniform atmospheric-pressure discharge in helium, *Phys. Plasmas*, 12 (2005), 023503.